



# PRODUCTION ENGINEERING ARCHIVES

ISSN 2353-5156 (print)  
ISSN 2353-7779 (online)

Exist since 4<sup>th</sup> quarter 2013  
Available online at [www.qpij.pl/production-engineering-archives](http://www.qpij.pl/production-engineering-archives)

## Microstructural features evaluation of age-hardened A 226 cast alloy by image analysis

Lenka Kuchariková<sup>1</sup>, Eva Tillová<sup>2</sup>

<sup>1</sup> University of Žilina, Faculty of Mechanical Engineering, Department of Materials Engineering, Univerzitná 8215/1, 010 26 Žilina, [lenka.kucharikova@fstroj.uniza.sk](mailto:lenka.kucharikova@fstroj.uniza.sk)

<sup>2</sup> University of Žilina, Faculty of Mechanical Engineering, Department of Materials Engineering, Univerzitná 8215/1, 010 26 Žilina.

### Article history

Received 11.09.2017  
Accepted 20.12.2017  
Available online 31.01.2018

### Keywords

age-hardening  
aluminum cast alloys  
image analysis  
quantitative analysis  
microstructural features

### Abstract

Age-hardening provides one of the most widely used mechanisms for the strengthening of aluminum alloys. The age-hardening involves three steps: solution treatment, quenching and aging. The temperature of solution treatment and aging is very important in order to reach desired properties of castings. The optimum temperature of solution treatment and aging led to formation microstructural features in form which does not lead to decreasing properties, but increasing ones. The major microstructural features in A 226 cast alloys which are responsible for increasing properties are: eutectic Si particles, Cu-rich phases, Fe-rich phases and porosity. The increase of properties depends on morphology, size and volume of microstructural features. In order to assess age-hardening influence on microstructural features in A226 cast alloys were used as possibilities of evaluation by means of image analysis. Quantitative analysis decelerate changes in microstructure includes the spheroidization and coarsening of eutectic silicon, gradual disintegration, shortening and thinning of Fe-rich intermetallic phases, the dissolution of precipitates and the precipitation of finer hardening phase (Al<sub>2</sub>Cu) further increase in the hardness and tensile strength in the alloy. Changes of mechanical properties were measured in line with STN EN ISO.

## 1. Introduction

Al-Si alloys are frequently used for many components in the automotive industry due to their excellent castability, good mechanical properties, machinability and wear resistance (LI R. X., ET AL. 2004; GROSSELLE F., ET AL. 2010). The recycled Al-Si-Cu alloys are extensively used to reduce materials cost compared to pure alloys. The alloys of the Al-Si-Cu system have become increasingly important in recent years, mainly in the automotive industry that uses recycled (secondary) aluminum for production of various motor mounts, engine parts, cylinder heads, pistons and so on (LI R.X., ET AL. 2004; RIOS C. T., ET AL. 2003). Al-Si-Cu alloys usually contain Cu (2-4 %), a certain amount of Fe, Mn, Mg and Zn that are present either undeliberate, or they are added deliberately to provide special material properties. These elements partly go into solid solution in the matrix and partly form intermetallic phases (GROSSELLE F., ET AL. 2010; RIOS C.T., ET AL. 2003).

The remelting of recycled metal saves almost 95% of the energy needed to produce prime aluminum from ore, and,

thus, triggers associated reductions in pollution and greenhouse emissions from mining, ore refining, and melting. Increasing the use of recycled metal is also quite important from an ecological standpoint, since producing aluminum by recycling creates only about 5% as much CO<sub>2</sub> as by primary production (DAS S. K. 2006; DAS S. K., ET AL. 2010; SENČÁKOVÁ L., ET AL. 2007).

Mechanical properties of Al-Si alloys are largely dependent upon an appropriate heat treatment technology, prior to the use of T6 condition. The heat treatment T6 influence morphology of structural features and lead to better properties. This heat treatment consist of the following stages (SJÖLANDER E., ET AL. 2010; TASH M., ET AL. 2007; ABDULWAHAB M. 2008; JOHANSEN H. G. 1994; ROMANKIEWICZ R., ET AL. 2014, SHAHA S. K., ET AL. 2017):

1. Solution treatment, that is necessary to produce a solid solution. Production of a solid solution involves keeping the Aluminum alloy at sufficiently high temperature for such holding time, that provides dissolution of the undissolved or precipitated soluble phase constituents so as to attain a reasonable degree of homogeneity;

2. Rapid cooling, also called quenching, usually with water at the temperature of 40-60°C, to obtain a supersaturated solid solution of solute atoms and vacancies in solid solution;
3. The third step of T4 heat treatment is natural aging to obtain the desired mechanical properties of casting. For heat treatment T6 (age-hardening) it is artificial ageing at elevated temperature to force precipitation from the supersaturated solid solution.

The present study is a part of a larger research project, which was conducted to investigate and to provide a better understanding of mechanical properties and microstructure (Si morphology, Fe- and Cu-rich phases) in secondary (recycled) AlSi9Cu3. The work is focused on studying the effect of age-hardening on changes in microstructural features.

## 2. Experimental

As an experimental material secondary hypoeutectic AlSi9Cu3 alloy was used. The chemical analysis of AlSi9Cu3 cast alloy was carried out using an arc spark spectroscopy and is (wt. %): 9.4% Si, 2.4% Cu, 0.9% Fe, 0.28% Mg, 0.24% Mn, 1.0% Zn, 0.05% Ni, 0.04% Ti, 0.03% Sn, 0.09% Pb, remainder % Al. The secondary alloy (prepared by recycling of aluminum scrap) was received in the form of 12.5 kg ingots. The experimental material was molten into the chill (chill casting). The melting temperature was maintained at 760°C ± 5°C. The molten metal was purified with salt AlCu4B6 before casting and was not modified or grain refined.

The experimental material was heat treated with the following regime: solution treatment at 515°C with holding time 4 hours which involves dissolution of soluble phases. The second step was water quenching at 50°C and the third step was artificial aging at different temperatures of artificial aging (130, 150, 170, 190 and 210°C with different holding times (2, 4, 8, 16 and 32 hours), where solute atoms precipitate.

From castings the testing samples for mechanical test (samples for measuring the ultimate tensile strength and samples for bending impact test) were made with dimensions corresponding to the standards.

In general, the AlSi9Cu3 cast alloy has lower corrosion resistance and is suitable for high temperature applications (dynamic exposed casts, where are not so big requirements on mechanical properties) that is max. 250°C. The AlSi9Cu3 alloy has the following technological properties: tensile strength (240-310 MPa), offset 0.2% yield stress (140-240 MPa), however, the low ductility limits (0.5-3%) and hardness HB 80-120. Hardness measurement of experimental material was performed by a Brinell hardness tester with a load of 62.5 Kp, 2.5 mm diameter ball and a dwell time of 15s (STN EN ISO 6506-1). The Brinell hardness value at each state was obtained as an average value of at least six measurements. Tensile properties were measured on the test machine ZDM 30 at room temperature (STN EN ISO 6892-1). A minimum number of five test specimens from each state (untreated and T6 heat treated) were used for tensile test.

For the microstructural features evolution quantitative analysis was used. Quantitative metallography (VAŠKO A., ET AL. 2014) was carried out on an Image Analyzer NIS – Elements to quantify the microstructural features (average volume and average size by magnification 100 and 500 x). Metallographic samples for the study were cut from the selected tensile test specimens (after testing) and hot mounted for metallographic preparation. The microstructures were studied using an optical microscope Neophot 32 (upon black-white etching). The samples were prepared by standard metallographic procedures (wet ground on SiC papers, DP polished with 3 µm diamond pastes followed by Struers Op-S and etched by standard etching solution Dix-Keller for optical microscope study.

## 3. Results and discussion

The results of hardness measurements are shown in Diagram 1. This diagram shows an obvious age-hardening phenomenon for each curve. At the early stage of aging for temperature 130 and 150°C the hardness increases with aging time until reaches the first peak (after 4 h). At intermediate stage of aging, after a little decrease the hardness increases again and reaches the potential second peak for temperature 130 and 150°C after 32 h. The final stage of aging, when the hardness decreases as a result of over-aging, was not observed. For samples aged at temperature 170°C a single aging peak after 8 hours and next a hardness high plateau from 8 to 32 hours was measured. The early stage of aging for temperature 190°C by 4 hours and 210°C by 2 hours was measured. The second aging peak for temperature 190°C by 16 hours was observed. For temperature 210°C the final stage of aging, when the hardness decreases as a result of over-aging, was not observed. The age-hardening peaks are correlated to their precipitation sequence. The first hardness peak of age-hardening curve is attained depending on the high density GP zones (especially GP II zones), while the second one is acquired in terms of metastable particles. The aging plateau corresponds to the continuous transition from GP zones to metastable phases. Highest Brinell hardness was 140 HBS for 515°C / 4 hours and artificial aging 170°C / from 8 to 32 hours.

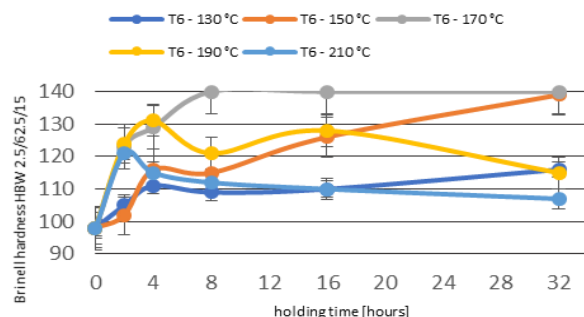


Diagram 1. Changes of Brinell hardness

In order to investigate the double-peak phenomenon of the AlSi9Cu3 alloy, tensile properties of the alloy aged at 130,

150, 170, 190 and 210°C for different times have been measured. The results are shown in Diagram 2. It can be found that the double aging peaks occurred for temperature 130, 150 and 170°C measured, but for temperature 190 and 210°C there was only one aging peak measured. For temperature 130, 150 and 170°C it was observed that the first aging peak occurred after holding time 4 hours. The second aging peak we observed after holding time 16 hours. For temperature 190°C we observed the first aging peak after 16 hours and for temperature 210°C after 8 hours. Highest strength tensile was 211 MPa for 515°C / 4 hours and artificial aging 170°C / from 16 hours.

The mechanical properties of cast component are determined largely by the shape and distribution of microstructural features. Therefore, quantitative analysis was used for their control. Optimum tensile, impact and fatigue properties are obtained with small, spherical and evenly distributed particles.

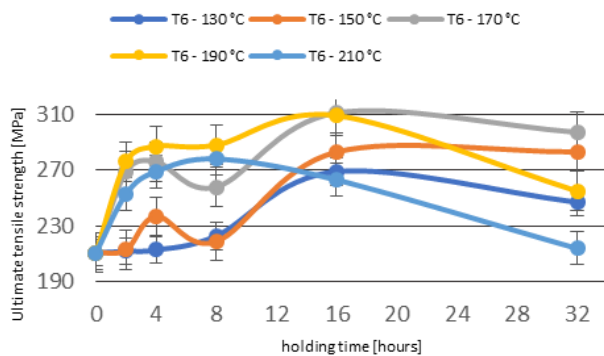


Diagram 2. Changes of ultimate tensile strength

The evolution of the Fe-rich phases during age-hardening is described in Fig. 4. In the as-cast state phase  $Al_{15}(FeMn)_3Si_2$  has a compact skeleton like form (Fig. 4a). The  $Al_{15}(FeMn)_3Si_2$  phase was shortened and fragmented to smaller skeleton particles during age-hardening (Fig. 4b-f).

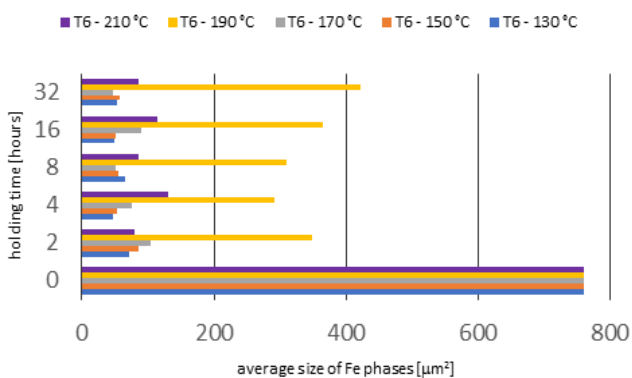


Diagram 3. Quantitative analysis of average size of Fe-rich phases

The influence of age-hardening on Fe-phase morphology was described by means of quantitative metallography to quantify average volume and size of  $Al_{15}(FeMn)_3Si_2$  phases (Diagrams 3 and 4). Maximum average size of Fe-rich phases

was observed at as-cast state (without heat treatment) 761  $\mu m^2$ . Minimum average size of Fe-rich phases (less than 50  $\mu m^2$ ) was observed after age-hardening by holding time greater than or equal to 4 hours independently from temperature of artificial aging (130, 150 or 170°C). The higher temperature of artificial aging leads to the increasing size of Fe-rich particles (190°C) (Diagram 3). The average volume of Fe-rich particles decreases with age-hardening, but temperature of artificial aging 190°C leads to increasing the volume (Fig. 5). The minimum volume was observed at 130 and 170°C (from 1.9 to 3.2%).

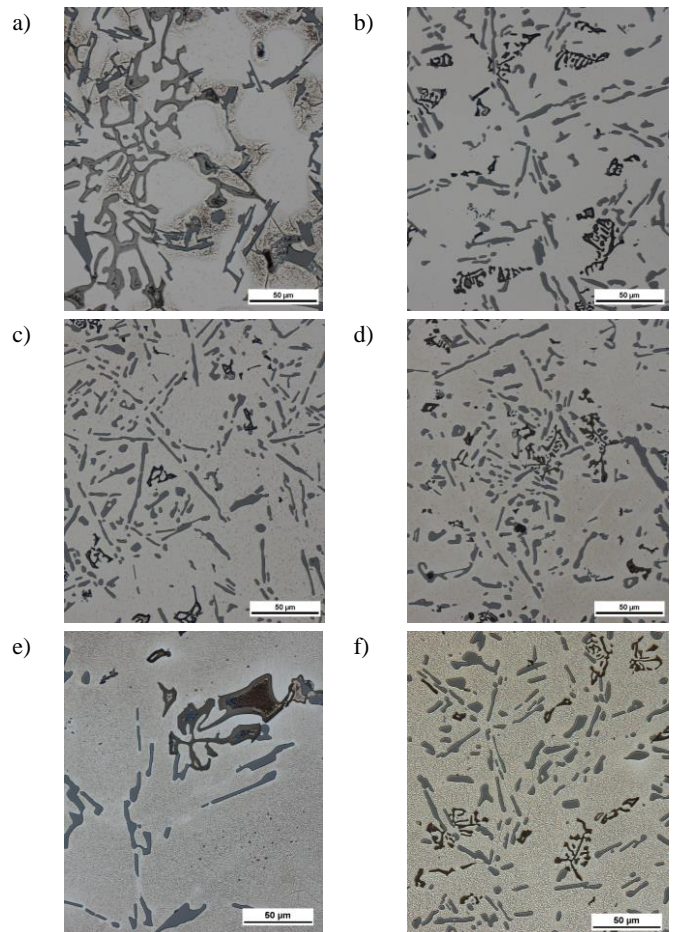


Fig. 4. Changes of Fe-rich phases and Si particles morphology during age-hardening after holding time 16 hours on temperature of artificial aging.

a) as-cast state; b) T6-130°C; c) T6-150°C; d) T6-170°C; e) T6-190°C; f) T6-210°C.

The effect of age-hardening – T6 on morphology of eutectic Si is demonstrated in Fig. 4, 8. The morphology changes of eutectic Si observed after age-hardening are documented for holding time 16 hours. Eutectic Si without heat treatment occurs in needles form (Fig. 4a). After heat treatment in every temperature of artificial aging it was observed that the Si platelets were fragmented in to smaller particles with rounded edge (Fig. 4b-f, 8b-f).

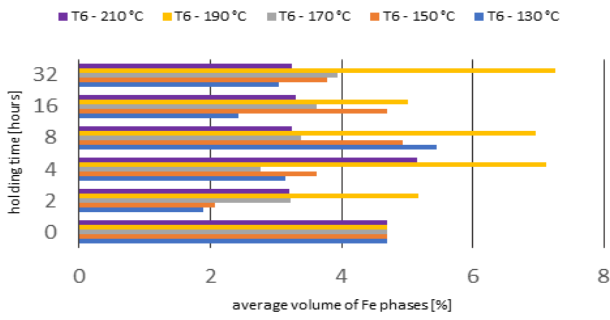


Fig. 5. Quantitative analysis of average volume of Fe-rich phases

Quantitative analysis of Si particles shows that the average size of eutectic Si particles obtained in heat treated samples decreases (727  $\mu\text{m}^2$  in as-cast state) with increasing of artificial aging, the most at 170°C (Fig. 6). Minimum value of average eutectic Si particles was observed at temperature of artificial aging 170°C with holding time 4 hours (41.75  $\mu\text{m}^2$ ). The average volume of Si particles was from 7.4 to 10% on metallographic samples (Fig. 7). The age-hardening markedly did not affect the volume of Si particles in microstructure of experimental material. The quantitative analysis decelerates great changes in size of Si particles.

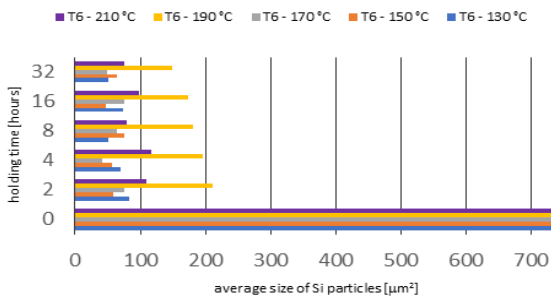


Fig. 6. Quantitative analysis of average size of Si particles

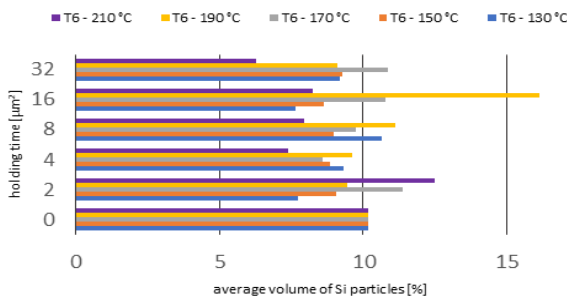


Fig. 7. Quantitative analysis of average volume of Si particles

From Cu rich phases were observed phases Al-Al<sub>2</sub>Cu-Si in microstructure of experimental material. This phase without T6 treatment occurs in form compact oval troops (Fig. 8a). After age-hardening compact Al-Al<sub>2</sub>Cu-Si phase disintegrates to separates Al<sub>2</sub>Cu particles or fibers (Fig. 8b-f).

The quantitative analysis was very hard, but the results show the correct information about dissolution of Cu rich phases during age-hardening (Fig. 9 and 8).

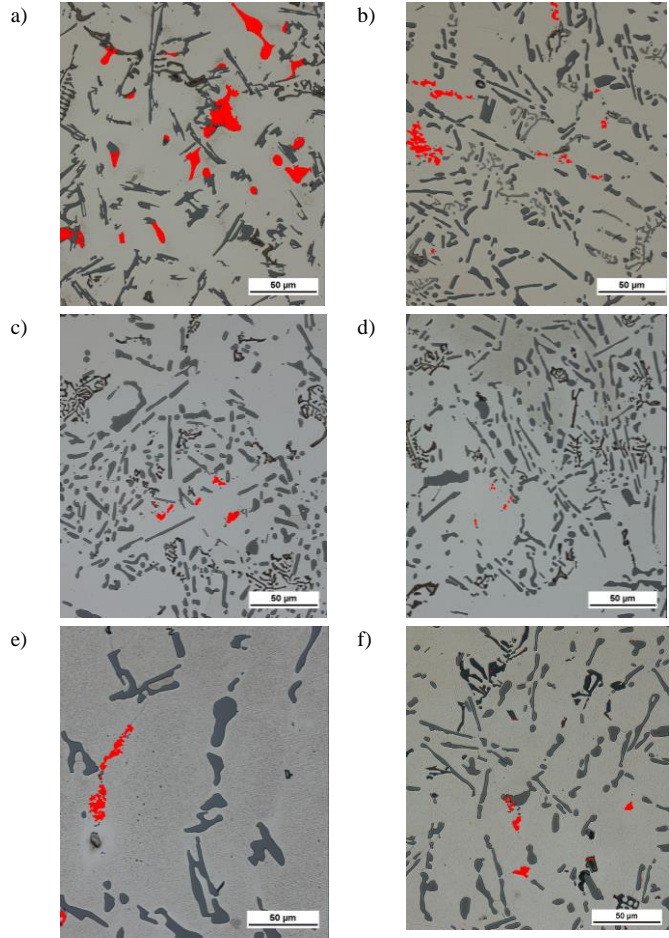


Fig. 8. Changes of Cu-rich phases and Si particles morphology during age-hardening after holding time 16 hours on temperature of artificial aging.

a) as-cast state; b) T6-130°C; c) T6-150°C; d) T6-170°C; e) T6-190°C; f) T6-210°C.

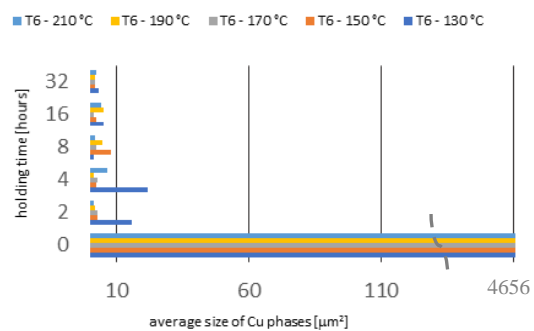


Fig. 9. Quantitative analysis of average size of Cu-rich phases

The amount of these phases was not corrected visibly on optical microscope because these phases were in a form of small particles or it was dissolved in the matrix. Maximum value of the average size of Cu-rich phases was measured in as-cast state (4656  $\mu\text{m}^2$ ) and minimum average area was estimated by age-hardening at temperature 170°C with holding time 16 hours (1.531  $\mu\text{m}^2$ ).

The volume of Cu rich phases in microstructure decreases with temperature of age-hardening and holding time, too (Fig. 10). The minimum volume was observed on samples after 150 and 170°C from 0.04 to 0.47%.

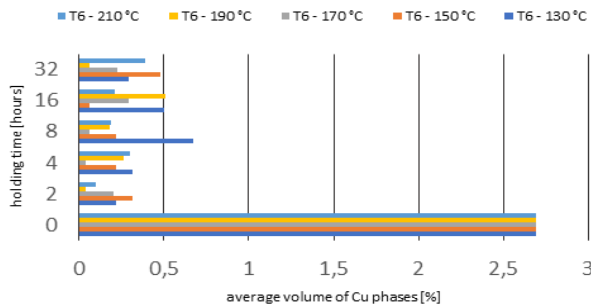


Fig. 10. Quantitative analysis of average volume of Cu-rich phases

#### 4. Summary and conclusion

The study of the microstructural features morphology changes during age-hardening evaluated with image analysis results in:

The mechanical properties (Brinell hardness and tensile strength) increase after age-hardening for all artificial temperatures. In the hardness age-hardening curve single aging peak (at 4 h) and hardness plateau (at 16 h) are present. In the tensile strength age-hardening curve the double-peak phenomenon (at 4h and at 16h) are observed.

The „optimum" schedule for mechanical properties is as follows: solution treatment: 4 h at 515°C; water quenching at 40°C; artificial aging: 16 h at 170°C. This will produce the following properties: HBW was in comparison with untreated state of 29% higher and strength tensile was of 32% higher.

In AlSi9Cu3 cast alloy were observed Fe-rich phases  $Al_{15}(FeMn)_3Si_2$ . Skeleton-like  $Al_{15}(FeMn)_3Si_2$  phase was dominant owing to the presence of Mn. The age-hardening caused changes of Fe-rich phases. Skeleton-like  $Al_{15}(FeMn)_3Si_2$  phases are dissolved and fragmented into small particles (average area reduces from 761 to 47  $\mu m^2$ ).

The age-hardening caused changes of Cu-rich intermetallic phases too. Compact Al-Al<sub>2</sub>Cu-Si eutectic are fragmented, dissolved and next redistributed within  $\alpha$ -matrix. The dissolution of Cu-rich phases during hardening holding increases the concentration of Cu and other alloying elements (Mg, Si) in the aluminum matrix.

The heat treatment caused changes of eutectic Si. The Si-platelets were fragmented in to smaller particles. In some volume of microstructure were observed spheroidized particles, which probably relate with temperature of solution treatment.

#### Acknowledgements

The authors acknowledge the VEGA N°1/0533/15, KEGA 049ŽU-4/2017 for the financial support of this work.

#### Reference

- ABDULWAHAB M. 2008. *Studies of the Mechanical Properties of Age-hardened Al-Si-Fe-Mn Alloy*. Australian Journal of Basic and Applied Sciences, Vol. 2 (4), 839-843.
- DAS S. K. 2006. *Designing Aluminum Alloys for a Recycling Friendly World*. Materials Science Forum, Vol. 519-521, 1239-1244.
- DAS K.S., GREN J. A. S. 2010. *Aluminum Industry and Climate Change-Assessment and Responses*. Jom, Vol. 62 (2), 27-31.
- GROSSELLE, F., TIMELLI G., BONOLLO F. 2010. *Doe applied to microstructural and mechanical properties of Al-Si-Cu-Mg casting alloys for automotive applications*. Materials Science and Engineering A 527, 3536-3545.
- JOHANSEN H. G. 1994. *Structural Aluminum Materials*. TALAT Lecture 2202 - Basic Level, 2-28.
- LI R. X., LI R. D., HE L. Z., LI C. X., GRUAN H. R., HUET Z. Q. 2004. *Age hardening behavior of cast Al-Si base alloy*, Materials Letters, 58, 2096-2101.
- RIOS C.T., CARAM R., BOLFORINI C., BOTTA F. W. J., KIMINAMI C. S. 2003. *Intermetallic compounds in the Al-Si-Cu system*. Acta microscopia, 12, 77-82
- ROMANKIEWICZ R., ROMANKIEWICZ F. 2014. *The influence of modification for structure and impact resistance of silumin AlSi11*. Production Engineering Archives, Vol. 3 (2), 6-9.
- SHAHA S.K., ET AL. 2017. *Ageing characteristics and high-temperature tensile properties of Al-Si-Cu-Mg alloys with micro-additions of Mo and Mn*. Materials Science and Engineering A. Vol. 684, 726-736.
- SENČÁKOVÁ L., VIRČIKOVÁ E. 2007. *Life cycle assessment of primary aluminum production*. Acta Metallurgica Slovaca, Vol. 13 (3), 412-419
- SJÖLANDER E., SEIFEDDINE S. 2010. *The heat treatment of Al-Si-Cu-Mg casting alloys*. Journal of Materials Processing Technology, Vol. 210 (10), 1249-1259.
- STN EN ISO 6892-1:2010 (42 0310). *Metallic materials. Tensile testing. Part 1: Method of test at ambient temperature*.
- STN EN ISO 6506-1:2015 (42 0371). *Metallic materials. Brinell hardness. Part 1: Test method*.
- TASH M., SAMUEL H. F., MUCCIARDI F., DOTY W. H. 2007. *Effect of metallurgical parameters on the hardness and microstructural characterization of as-cast and heat-treated 356 and 319 aluminum alloys*. Materials Science and Engineering A443, 185-201.
- VÁŠKO A., MARKOVIČOVÁ M., ZATKALÍKOVÁ V., TILLOVÁ E. 2014. *Quantitative evaluation of microstructure of graphitic cast irons*. Manufacturing technology, Vol. 14 (3), 478-182.

---

## 时效硬化的 A 226 铸造合金的显微组织特征评价

---

### 關鍵詞

时效硬化  
铝铸造合金  
图像分析  
定量分析  
显微结构特征

### 摘要

时效硬化提供了加强铝合金使用最广泛的机制之一。时效硬化包括三个步骤：固溶处理，淬火和老化。为了达到所需的铸件性能，固溶处理和老化的温度是非常重要的。固溶处理和时效处理的最佳温度导致形成的微观结构特征不会导致性能下降，反而会增加。A 226 铸造合金的主要显微组织特征是共晶 Si 颗粒，富 Cu 相，富 Fe 相和孔隙率。性能的增加取决于微观结构特征的形态，大小和体积。为了评估时效硬化对 A226 铸造合金显微组织特征的影响，通过图像分析的方法作为评估的可能性。定量分析减速组织变化包括共晶硅的球化和粗化，逐渐分解，富 Fe 金属间化合物的缩短和变薄，析出物的溶解和较细的硬化相（Al<sub>2</sub>Cu）的析出进一步增加了硬度和抗拉强度在合金中。根据 STN EN ISO 测量机械性能的变化。

---